

Supporting Information

Strong and Anisotropic Superexchange in the Single-Molecule Magnet (SMM) $[\text{Mn}^{\text{III}}_6\text{Os}^{\text{III}}]^{3+}$: Promoting SMM Behavior through 3d-5d Transition Metal Substitution

**Veronika Hoeke,[†] Anja Stammeler,[†] Hartmut Bögge,[†] Jürgen Schnack,^{*,#}
Thorsten Glaser^{*,†}**

[†] *Lehrstuhl für Anorganische Chemie I, Fakultät für Chemie, Universität Bielefeld, Universitätsstr. 25, D-33615 Bielefeld, Germany*

[#] *Fakultät für Physik, Universität Bielefeld, Universitätsstr. 25, D-33615 Bielefeld, Germany*

^{*} To whom correspondence should be addressed. E-mail: thorsten.glaser@uni-bielefeld.de (T.G.), jschnack@uni-bielefeld.de (J.S.)

Synthesis and Characterization

In analogy to the synthesis of the heptanuclear triplesalen complexes $[\text{Mn}^{\text{III}}_6\text{Cr}^{\text{III}}]^{3+}$,^{1,2} $[\text{Mn}^{\text{III}}_6\text{Fe}^{\text{III}}]^{3+}$,^{3,4} $[\text{Mn}^{\text{III}}_6\text{Co}^{\text{III}}]^{3+}$,⁵ and $[\text{Mn}^{\text{III}}_6\text{Mn}^{\text{III}}]^{3+}$,^{6,7} we reacted $\text{H}_6\text{talen}^{\text{tBu}_2}$, $\text{Mn}^{\text{II}}(\text{OAc})_2 \cdot 4\text{H}_2\text{O}$, and $(\text{Ph}_4\text{P})_3[\text{Os}^{\text{III}}(\text{CN})_6]$ in the molar ratio 2.0 : 5.7 : 1.0 in methanol with the aim of generating $[\text{Mn}^{\text{III}}_6\text{Mn}^{\text{III}}]^{3+}$. Addition of a large excess of $\text{NaClO}_4 \cdot \text{H}_2\text{O}$ resulted in the instantaneous formation of a colorless precipitate, which was removed from the reaction mixture by filtration and identified as $(\text{Ph}_4\text{P})\text{ClO}_4$ by FT-IR spectroscopy. Slow evaporation of the solvent from the filtrate led to the formation of brown crystals. While elemental analysis provided no indication for an inhomogeneity of these batches, their visual inspection revealed that they contained crystals of different morphology. The majority of crystals are best described as rhombs, which were analyzed by single-crystal X-ray diffraction as $\{[(\text{talen}^{\text{tBu}_2})(\text{Mn}^{\text{III}}(\text{MeOH}))_3]_2\{\text{Os}^{\text{III}}(\text{CN})_6\}(\text{ClO}_4)_3 \cdot 12\text{MeOH}\}$, while some small needles were also found as a minor component, which were not suitable for single-crystal X-ray diffraction analysis.

FT-IR spectra of the mixture of crystals measured as KBr pellets reveal the presence of the typical vibrations of the ligand $(\text{talen}^{\text{tBu}_2})^{6-}$ in the heptanuclear complexes $[\text{Mn}^{\text{III}}_6\text{M}^{\text{c}}]^{3+}$ ¹⁻⁷ as well as those of the ClO_4^- counterion. Additionally, characteristic bands for the $\nu(\text{C}\equiv\text{N})$ vibration appear in the 2120-2020 cm^{-1} region, namely two bands of medium intensity at 2112 and 2058 cm^{-1} and one weak but very sharp band at 2025 cm^{-1} . In analogy to the spectra of $[\text{Mn}^{\text{III}}_6\text{Cr}^{\text{III}}]^{3+}$,^{1,2} $[\text{Mn}^{\text{III}}_6\text{Co}^{\text{III}}]^{3+}$,⁵ and $[\text{Mn}^{\text{III}}_6\text{Mn}^{\text{III}}]^{3+}$,^{6,7} only one band for the symmetric $\nu(\text{C}\equiv\text{N})$ vibration of the bridging $[\text{Os}^{\text{III}}(\text{CN})_6]^{3-}$ unit is expected, which should exhibit a shift to higher energies compared to the ionic $[\text{Os}^{\text{III}}(\text{CN})_6]^{3-}$. FT-IR spectra of $(\text{Ph}_4\text{P})_3[\text{Os}^{\text{III}}(\text{CN})_6]$ in KBr show four bands at 2097, 2079, 2039, and 2025 cm^{-1} , with the two bands at lower energy virtually coinciding with the two strongest bands in the IR spectrum of $\text{K}_4[\text{Os}^{\text{II}}(\text{CN})_6]$ at 2043 and 2027 cm^{-1} . In contrast, the spectrum of $(\text{Ph}_4\text{P})_3[\text{Os}^{\text{III}}(\text{CN})_6]$ in nujol exhibits only one strong band at 2077 cm^{-1} and a very weak but sharp band at 2097 cm^{-1} . These data indicate a reduction of the ionic $[\text{Os}^{\text{III}}(\text{CN})_6]^{3-}$ by Br^- of the KBr pellet in analogy to $[\text{Fe}^{\text{III}}(\text{CN})_6]^{3-}$,⁴ which is corroborated by the lack of reproducibility of the relative intensities of the four bands observed for $(\text{Ph}_4\text{P})_3[\text{Os}^{\text{III}}(\text{CN})_6]$ in different KBr pellets due to variations in the grinding time of the sample with KBr. In order to probe the possible reduction of $[\text{Mn}^{\text{III}}_6\text{Os}^{\text{III}}]^{3+}$ by Br^- of the KBr pellet in analogy to $[\text{Mn}^{\text{III}}_6\text{Fe}^{\text{III}}]^{3+}$,^{3,4} we have measured IR spectra of the mixture of crystals obtained by

the above-mentioned procedure after grinding the crystals with KBr for a first FT-IR measurement and then re-grinding the components of the KBr pellet for a second measurement. Interestingly, the intensity of the band at 2112 cm⁻¹ decreases with prolonged grinding, while the band at 2058 cm⁻¹ exhibits an intensity increase. This indicates that **[Mn^{III}₆Os^{III}]³⁺** is indeed reduced by Br⁻ of the KBr pellet, which is in line with the half-wave potential $E_{1/2} = 0.07$ V vs Fc⁺/Fc of the Os^{III}/Os^{II} couple as determined by cyclic and square-wave voltammetry (*vide infra*), and provides strong evidence for an assignment of the bands at 2112 cm⁻¹ and 2058 cm⁻¹ to the symmetric $\nu(\text{C}\equiv\text{N})$ vibrations of the bridging [Os^{III}(CN)₆]³⁻ and [Os^{II}(CN)₆]⁴⁻ units in **[Mn^{III}₆Os^{III}]³⁺** and **[Mn^{III}₆Os^{II}]²⁺**, respectively. The shift of these bands to higher energies compared to the respective ionic [Os^{III/II}(CN)₆]^{3-/4-} is consistent with the symmetric bridging mode of the central hexacyanometallate as found in other **[Mn^{III}₆M^c]ⁿ⁺** complexes.¹⁻⁷

The IR spectrum of the mixture of crystals in nujol exhibits not only a band at 2112 cm⁻¹, but also a band of lower intensity at 2058 cm⁻¹. The previous analysis of the KBr spectra in conjunction with the observation of different kinds of crystals in the investigated samples provides strong evidence for an assignment of the low-intensity band to **[Mn^{III}₆Os^{II}]²⁺** resulting from the *in situ* reduction of an Os^{III} species during the synthetic procedure. However, the band may also originate from **[Mn^{III}₆Os^{III}]³⁺** in analogy to **[Mn^{III}₆Fe^{III}]³⁺**, for which two bands at 2133 and 2060 cm⁻¹ in the IR spectrum in nujol were assigned to the bridging [Fe^{III}(CN)₆]³⁻, as Mössbauer spectroscopy provided no indication for the presence of an Fe^{II} species.⁴

In order to ensure the isolation of pure batches of **[Mn^{III}₆Os^{III}](ClO₄)₃**, and to elucidate the origin of the band at 2058 cm⁻¹ in the IR spectra of the inhomogeneous batches of crystals in nujol, we recrystallized these batches while adding a suitable oxidizing agent. In view of the redox potential of the Os^{III}/Os^{II} couple in **[Mn^{III}₆Os^{III}]³⁺** (*vide supra*), and considering the perchlorate counterion, we employed [(tacn)₂Ni^{III}](ClO₄)₃ (tacn = 1,4,7-triazacyclononane), which exhibits a half-wave potential $E_{1/2} = 0.55$ V vs Fc⁺/Fc of the Ni^{III}/Ni^{II} couple.⁸ Upon re-suspending the mixture of crystals obtained by the above-mentioned procedure in methanol, a small brown residue remained even after prolonged stirring and further addition of solvent. FT-IR spectra of the residue in KBr and nujol show a strong band at 2058 cm⁻¹, while the spectrum in KBr additionally exhibits very weak but sharp bands at 2112 and 2025 cm⁻¹. The strong band at 2058 cm⁻¹ confirms the presence of **[Mn^{III}₆Os^{II}]²⁺** in the inhomogeneous

batches of crystals. The filtrate was treated with a solution of $[(\text{tacn})_2\text{Ni}^{\text{III}}](\text{ClO}_4)_3$ in acetonitrile, as this salt is insoluble in methanol. Slow evaporation of the solvent afforded a brown microcrystalline solid, which exhibits a band at 2112 cm^{-1} in its FT-IR spectrum in nujol, whereas the previously observed band at 2058 cm^{-1} is absent. This allows a definite assignment of the latter to $[\text{Mn}^{\text{III}}_6\text{Os}^{\text{II}}]^{2+}$ with no contribution from $[\text{Mn}^{\text{III}}_6\text{Os}^{\text{III}}]^{3+}$. As expected, the IR spectrum of the product in KBr shows three bands at 2112 , 2058 , and 2025 cm^{-1} , with the latter two exhibiting a lower intensity compared to the spectra of the inhomogeneous batches of crystals that were measured after a similar grinding time of the sample with KBr. Batches obtained from recrystallization with addition of $[(\text{tacn})_2\text{Ni}^{\text{III}}](\text{ClO}_4)_3$ were used to further characterize $[\text{Mn}^{\text{III}}_6\text{Os}^{\text{II}}](\text{ClO}_4)_3$.

For purposes of comparison with $[\text{Mn}^{\text{III}}_6\text{Os}^{\text{III}}]^{3+}$, and with the aim of definitely assigning the small brown needles found as a minor component in our first batches (*vide supra*) to $[\text{Mn}^{\text{III}}_6\text{Os}^{\text{II}}](\text{ClO}_4)_2$, we tried to synthesize this compound in an analytically pure form. The reaction of $\text{H}_6\text{talen}^{\text{tBu}_2}$, $\text{Mn}^{\text{II}}(\text{OAc})_2 \cdot 4\text{H}_2\text{O}$, and $[\text{K}(18\text{-crown-6})]_4[\text{Os}^{\text{II}}(\text{CN})_6]$, with the latter being generated *in situ* from $\text{K}_4[\text{Os}^{\text{II}}(\text{CN})_6]$ and 18-crown-6 in analogy to the syntheses of $[\text{Mn}^{\text{III}}_6\text{Fe}^{\text{III}}]^{3+}$ ^{3,4} and $[\text{Mn}^{\text{III}}_6\text{Co}^{\text{III}}]^{3+}$,⁵ in the molar ratio 2.0 : 5.6 : 1.0 in methanol yielded indeed small brown needles after addition of $\text{NaClO}_4 \cdot \text{H}_2\text{O}$. The needles had the same morphology as those obtained as a minor component when starting from $(\text{Ph}_4\text{P})_3[\text{Os}^{\text{III}}(\text{CN})_6]$ and were again not suitable for single-crystal X-ray diffraction studies. FT-IR spectra of the needles in KBr and nujol exhibit a very strong band at 2058 cm^{-1} , while the spectrum in KBr additionally shows a weak but very sharp band at 2025 cm^{-1} , which is also attributed to $[\text{Mn}^{\text{III}}_6\text{Os}^{\text{II}}]^{2+}$.

However, with prolonged evaporation of solvent, some rhombs also appeared, which were analyzed as $\{[(\text{talen}^{\text{tBu}_2})(\text{Mn}^{\text{III}}(\text{MeOH}))_3]_2\{\text{Os}^{\text{III}}(\text{CN})_6\}\}(\text{ClO}_4)_3 \cdot 12\text{MeOH}$ by single-crystal X-ray diffraction. Concomitantly, a small band at 2112 cm^{-1} was detected in the FT-IR spectra of the product in KBr and nujol, indicating the presence of $[\text{Mn}^{\text{III}}_6\text{Os}^{\text{III}}]^{3+}$ resulting from the *in situ* oxidation of an Os^{II} species. With the aim of obtaining pure batches of $[\text{Mn}^{\text{III}}_6\text{Os}^{\text{II}}](\text{ClO}_4)_2$, we performed the reaction under an argon atmosphere, which successfully afforded $\{[(\text{talen}^{\text{tBu}_2})\text{Mn}^{\text{III}}]_3\}_2\{\text{Os}^{\text{II}}(\text{CN})_6\}(\text{ClO}_4)_2 \cdot 5\text{MeOH} \cdot 10\text{H}_2\text{O}$ in a high yield (73%). The high solvent content was confirmed by elemental analysis on different batches and is in line with the results of single-crystal X-ray diffraction and elemental analysis on other $[\text{Mn}^{\text{III}}_6\text{M}^{\text{c}}]^{n+}$ compounds,

which generally crystallize with a large number of solvent molecules of crystallization in addition to frequently carrying solvent molecules at the sixth coordination sites of the terminal Mn^{III} ions.¹⁻⁷

In addition to the differences relating to the $\nu(\text{C}\equiv\text{N})$ vibrations (*vide supra*), the FT-IR spectra of **[Mn^{III}₆Os^{III}]³⁺** and **[Mn^{III}₆Os^{II}]²⁺** exhibit some notable differences with respect to characteristic bands of the ligand (talent^{t-Bu₂})⁶⁻. Interestingly, these differences seem to be universal for **[Mn^{III}₆M^c]³⁺** trications *versus* **[Mn^{III}₆M^c]²⁺** dications, as evident from comparison of the spectra of a series of **[Mn^{III}₆M^c]ⁿ⁺** complexes (M^c = Fe^{II}, Os^{II}, Mn^{III}, Cr^{III}, Co^{III}, Fe^{III}, Os^{III}) (Fig. 1). The IR spectra of the tricationic **[Mn^{III}₆M^c]³⁺** complexes show prominent bands at 1611, 1570, 1535, and 1491 cm⁻¹, with the band at lowest energy being strongest in intensity. The respective region in the spectra of the **[Mn^{III}₆M^c]²⁺** dications also shows four bands. While virtually no change compared to the **[Mn^{III}₆M^c]³⁺** trications is observed for the three bands at higher energy, the band at lowest energy shifts to 1497 cm⁻¹ with a simultaneous decrease in intensity. Importantly, this band has been identified as a signature of the heteroradialene character of the central phloroglucinol backbone (*vide infra*) and most likely originates from vibrational modes with a pronounced C=O stretching character.^{9,10}

ESI mass spectra of **[Mn^{III}₆Os^{III}](ClO₄)₃** in the positive ion mode show a signal at a mass-to-charge-ratio m/z of 963 with mass and isotope distribution pattern corresponding to the trication **[{(talent^{t-Bu₂})Mn₃]₂{Os(CN)₆}]³⁺**. Additionally, the dications **[{(talent^{t-Bu₂})Mn₃]₂{Os(CN)₆}(H₂O)_n]²⁺** ($n = 0, 1, 2, 6$) are detected at $m/z = 1444, 1452, 1461, \text{ and } 1493$. In contrast, ESI mass spectra of **[Mn^{III}₆Os^{II}](ClO₄)₂** in the respective m/z range exhibit only the dication **[{(talent^{t-Bu₂})Mn₃]₂{Os(CN)₆}]²⁺**. In addition, the monocations **[{(talent^{t-Bu₂})Mn₃]₂{Os(CN)₆}(H₂O)_n]⁺** ($n = 0, 2$) are detected at $m/z = 2887$ and 2923 . The appearance of species carrying solvent molecules at the sixth coordination sites of some terminal Mn^{III} ions in the mass spectra is rather unusual for our heptanuclear **[Mn^{III}₆M^c]ⁿ⁺** compounds.¹⁻⁷ MALDI-TOF mass spectra of **[Mn^{III}₆Os^{III}](ClO₄)₃** and **[Mn^{III}₆Os^{II}](ClO₄)₂** in the positive ion mode exhibit signals at $m/z = 2887, 2987, \text{ and } 3087$ attributable to the monocations **[{(talent^{t-Bu₂})Mn₃]₂{Os(CN)₆}(ClO₄)_n]⁺** ($n = 0, 1, 2$), which is in analogy to the respective spectra of **[Mn^{III}₆Cr^{III}](ClO₄)₃**,¹¹ and the signal of the dication **[{(talent^{t-Bu₂})Mn₃]₂{Os(CN)₆}]²⁺**.

Fig. S1. Thermal ellipsoid plot of the fragment of $[\text{Mn}^{\text{III}}_6\text{Os}^{\text{III}}]^{3+}$ in the asymmetric unit in crystals of **1** with the numbering scheme used. Thermal ellipsoids are drawn at the 50 % probability level; hydrogen atoms are omitted for clarity.

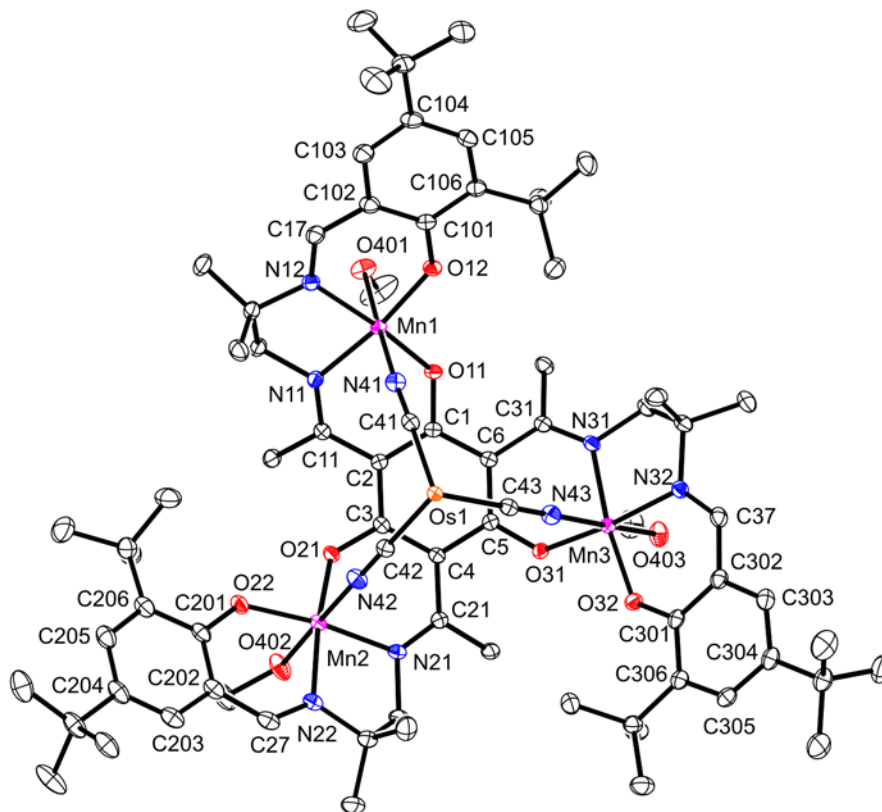


Table S1. Selected Interatomic Distances [Å] and Angles [deg] for **1**.

Mn(1)-O(11)	1.8876(13)	C(201)-C(202)	1.419(3)
Mn(1)-O(12)	1.8747(14)	C(201)-C(206)	1.424(3)
Mn(1)-N(11)	1.9791(16)	C(202)-C(203)	1.406(3)
Mn(1)-N(12)	1.9803(16)	C(203)-C(204)	1.374(3)
Mn(1)-N(41)	2.1817(17)	C(204)-C(205)	1.400(3)
Mn(1)-O(401)	2.3780(15)	C(205)-C(206)	1.394(3)
Mn(2)-O(21)	1.8918(13)	C(301)-C(302)	1.418(3)
Mn(2)-O(22)	1.8751(14)	C(301)-C(306)	1.423(3)
Mn(2)-N(21)	1.9856(16)	C(302)-C(303)	1.410(3)
Mn(2)-N(22)	1.9812(17)	C(303)-C(304)	1.378(3)
Mn(2)-N(42)	2.1919(17)	C(304)-C(305)	1.404(3)
Mn(2)-O(402)	2.3115(15)	C(305)-C(306)	1.391(3)
Mn(3)-O(31)	1.8975(13)	Mn(1)-Mn(2)	6.8082(5)
Mn(3)-O(32)	1.8707(14)	Mn(1)-Mn(3)	6.8467(5)
Mn(3)-N(31)	1.9789(16)	Mn(2)-Mn(3)	6.8897(5)
Mn(3)-N(32)	1.9838(16)	Os(1)-Mn(1)	5.3036(4)
Mn(3)-N(43)	2.1957(17)	Os(1)-Mn(2)	5.3292(4)
Mn(3)-O(403)	2.3338(15)	Os(1)-Mn(3)	5.3163(3)
O(11)-C(1)	1.310(2)	Os(1)-C(41)	2.048(2)
O(12)-C(101)	1.321(2)	Os(1)-C(42)	2.0486(19)
O(21)-C(3)	1.306(2)	Os(1)-C(43)	2.0493(19)
O(22)-C(201)	1.322(2)	N(41)-C(41)	1.152(3)
O(31)-C(5)	1.308(2)	N(42)-C(42)	1.151(3)
O(32)-C(301)	1.321(2)	N(43)-C(43)	1.151(3)
N(11)-C(11)	1.302(2)	O(12)-Mn(1)-O(11)	95.93(6)
N(12)-C(17)	1.290(3)	O(12)-Mn(1)-N(11)	171.06(6)
N(21)-C(21)	1.301(3)	O(11)-Mn(1)-N(11)	87.93(6)
N(22)-C(27)	1.288(3)	O(12)-Mn(1)-N(12)	91.84(6)
N(31)-C(31)	1.300(2)	O(11)-Mn(1)-N(12)	168.90(6)
N(32)-C(37)	1.291(3)	N(11)-Mn(1)-N(12)	83.30(7)
C(1)-C(2)	1.418(3)	O(12)-Mn(1)-N(41)	93.98(6)
C(1)-C(6)	1.425(3)	O(11)-Mn(1)-N(41)	90.65(6)
C(2)-C(3)	1.429(3)	N(11)-Mn(1)-N(41)	94.04(7)
C(3)-C(4)	1.424(3)	N(12)-Mn(1)-N(41)	96.74(7)
C(4)-C(5)	1.428(2)	O(12)-Mn(1)-O(401)	86.12(6)
C(5)-C(6)	1.420(3)	O(11)-Mn(1)-O(401)	86.98(5)
C(2)-C(11)	1.462(2)	N(11)-Mn(1)-O(401)	86.03(6)
C(17)-C(102)	1.440(3)	N(12)-Mn(1)-O(401)	85.63(6)
C(4)-C(21)	1.461(3)	N(41)-Mn(1)-O(401)	177.62(6)
C(27)-C(202)	1.439(3)	O(22)-Mn(2)-O(21)	96.00(6)
C(6)-C(31)	1.457(3)	O(22)-Mn(2)-N(22)	92.16(7)
C(37)-C(302)	1.432(3)	O(21)-Mn(2)-N(22)	169.47(7)
C(101)-C(102)	1.419(3)	O(22)-Mn(2)-N(21)	172.10(6)
C(101)-C(106)	1.422(3)	O(21)-Mn(2)-N(21)	88.04(6)
C(102)-C(103)	1.411(3)	N(22)-Mn(2)-N(21)	83.09(7)
C(103)-C(104)	1.378(3)	O(22)-Mn(2)-N(42)	95.03(6)
C(104)-C(105)	1.403(3)	O(21)-Mn(2)-N(42)	90.86(6)
C(105)-C(106)	1.393(3)	N(22)-Mn(2)-N(42)	95.06(7)
		N(21)-Mn(2)-N(42)	91.69(7)
		O(22)-Mn(2)-O(402)	86.60(6)

O(21)-Mn(2)-O(402)	87.48(6)
N(22)-Mn(2)-O(402)	86.36(6)
N(21)-Mn(2)-O(402)	86.79(6)
N(42)-Mn(2)-O(402)	177.79(6)
O(32)-Mn(3)-O(31)	96.14(6)
O(32)-Mn(3)-N(31)	172.31(6)
O(31)-Mn(3)-N(31)	88.96(6)
O(32)-Mn(3)-N(32)	91.37(6)
O(31)-Mn(3)-N(32)	170.13(6)
N(31)-Mn(3)-N(32)	82.95(7)
O(32)-Mn(3)-N(43)	94.50(6)
O(31)-Mn(3)-N(43)	89.28(6)
N(31)-Mn(3)-N(43)	91.30(6)
N(32)-Mn(3)-N(43)	96.51(7)
O(32)-Mn(3)-O(403)	89.50(6)
O(31)-Mn(3)-O(403)	85.08(6)
N(31)-Mn(3)-O(403)	85.20(6)
N(32)-Mn(3)-O(403)	88.60(6)
N(43)-Mn(3)-O(403)	173.41(6)
Os(1)-Mn(1)-Mn(2)	50.352(4)
Os(1)-Mn(1)-Mn(3)	49.938(5)
Os(1)-Mn(2)-Mn(1)	50.020(4)
Os(1)-Mn(2)-Mn(3)	49.588(4)
Os(1)-Mn(3)-Mn(1)	49.775(4)
Os(1)-Mn(3)-Mn(2)	49.752(4)
Mn(2)-Mn(1)-Mn(3)	60.603(5)
Mn(1)-Mn(2)-Mn(3)	59.974(5)
Mn(1)-Mn(3)-Mn(2)	59.422(4)
C(1)-O(11)-Mn(1)	124.56(12)
C(101)-O(12)-Mn(1)	130.93(13)
C(3)-O(21)-Mn(2)	123.76(12)
C(201)-O(22)-Mn(2)	130.84(13)
C(5)-O(31)-Mn(3)	125.32(12)
C(301)-O(32)-Mn(3)	130.96(13)
C(41)-Os(1)-C(42)	90.23(7)
C(41)-Os(1)-C(43)	91.60(7)
C(42)-Os(1)-C(43)	91.52(7)
Mn(1)-Os(1)-Mn(2)	79.628(5)
Mn(1)-Os(1)-Mn(3)	80.287(5)
Mn(3)-Os(1)-Mn(2)	80.660(6)
C(41)-N(41)-Mn(1)	159.70(15)
C(42)-N(42)-Mn(2)	161.92(16)
C(43)-N(43)-Mn(3)	158.97(16)
N(41)-C(41)-Os(1)	178.69(18)
N(42)-C(42)-Os(1)	179.26(18)
N(43)-C(43)-Os(1)	178.50(17)

Symmetry transformations used to generate equivalent atoms:

#1 -x+1,-y+1,-z+1 #2 -x+1,-y,-z+1

References

- (1) Glaser, T.; Heidemeier, M.; Weyhermüller, T.; Hoffmann, R.-D.; Rupp, H.; Müller, P. *Angew. Chem. Int. Ed.* **2006**, *45*, 6033-6037.
- (2) Hoeke, V.; Heidemeier, M.; Krickemeyer, E.; Stammler, A.; Bögge, H.; Schnack, J.; Postnikov, A.; Glaser, T. *Inorg. Chem.* **2012**, *51*, 10929-10954.
- (3) Hoeke, V.; Krickemeyer, E.; Heidemeier, M.; Theil, H.; Stammler, A.; Bögge, H.; Weyhermüller, T.; Schnack, J.; Glaser, T. *Eur. J. Inorg. Chem.* **2013**, 4398-4409.
- (4) Glaser, T.; Heidemeier, M.; Krickemeyer, E.; Bögge, H.; Stammler, A.; Fröhlich, R.; Bill, E.; Schnack, J. *Inorg. Chem.* **2009**, *48*, 607-620.
- (5) Krickemeyer, E.; Hoeke, V.; Stammler, A.; Bögge, H.; Schnack, J.; Glaser, T. *Z. Naturforsch.* **2010**, *65b*, 295-303.
- (6) Hoeke, V.; Gieb, K.; Müller, P.; Ungur, L.; Chibotaru, L. F.; Heidemeier, M.; Krickemeyer, E.; Stammler, A.; Bögge, H.; Schröder, C.; Schnack, J.; Glaser, T. *Chem. Sci.* **2012**, *3*, 2868-2882.
- (7) Hoeke, V.; Heidemeier, M.; Krickemeyer, E.; Stammler, A.; Bögge, H.; Schnack, J.; Glaser, T. *Dalton Trans.* **2012**, *41*, 12942-12959.
- (8) Wieghardt, K.; Schmidt, W.; Herrmann, W.; Kuppers, H. J. *Inorg. Chem.* **1983**, *22*, 2953-2956.
- (9) Feldscher, B.; Krickemeyer, E.; Moselage, M.; Theil, H.; Hoeke, V.; Kaiser, Y.; Stammler, A.; Bögge, H.; Glaser, T. *Sci. China: Chem.* **2012**, *55*, 951-966.
- (10) Frhr. v. Richthofen, C.-G.; Feldscher, B.; Lippert, K.-A.; Stammler, A.; Bögge, H.; Glaser, T. *Z. Naturforsch.* **2013**, *68b*, 64-86.
- (11) Helmstedt, A.; Sacher, M. D.; Gryzia, A.; Harder, A.; Brechling, A.; Müller, N.; Heinzmann, U.; Hoeke, V.; Krickemeyer, E.; Glaser, T.; Bouvron, S.; Fonin, M. *J. Electron Spectrosc. Relat. Phenom.* **2012**, *184*, 583-588.